

Core-level anionic photofragmentation of gaseous CCl₄ and solid-state analogsK. T. Lu,^{1,*} J. M. Chen,^{1,†} J. M. Lee,^{1,2} S. C. Haw,¹ T. L. Chou,¹ S. A. Chen,¹ and T. H. Chen¹¹*National Synchrotron Radiation Research Center (NSRRC), Hsinchu, 30076 Taiwan, Republic of China*²*Department of Electrophysics, National Chiao Tung University, Hsinchu, 30010 Taiwan, Republic of China*

(Received 11 May 2009; published 8 September 2009)

The dissociation dynamics of anionic and excited neutral fragments of gaseous CCl₄ and CCl₄ adsorbed on Si(100) ~90 K following Cl 2*p* core-level excitations were investigated on combining measurements of photon-induced anionic dissociation, x-ray absorption, and uv-visible dispersed fluorescence. The transitions of core electrons to high Rydberg states or doubly excited states near Cl 2*p* ionization thresholds of gaseous CCl₄ remarkably enhance the production of excited neutral fragments (C* and CCl*); this enhancement is attributed to the contribution from the shake-modified resonant Auger decay and/or postcollision interaction (PCI). The Cl⁻ anion is significantly reinforced in the vicinity of the Cl 2*p*_{1/2,3/2} ionization threshold of gaseous CCl₄, originating from PCI-mediated photoelectron recapture. The Cl 2*p* → 7*a*₁* excitation for CCl₄/Si(100) at ~90 K enhances the Cl⁻ desorption yield at a submonolayer level. This resonant enhancement of Cl⁻ yield at the 7*a*₁* resonance in the Cl 2*p* edge at a submonolayer level occurs through the formation of high-lying molecular-ion states of CCl₄ adsorbed on a Si surface.

DOI: [10.1103/PhysRevA.80.033406](https://doi.org/10.1103/PhysRevA.80.033406)

PACS number(s): 32.80.Hd, 78.70.Dm, 41.60.Ap

I. INTRODUCTION

Core-level spectroscopy, involving measuring the yields of electrons, photons, or ions as a function of photon energy in the region of a core-shell threshold, of gaseous molecules and molecular adsorbates on surfaces using synchrotron radiation have been subjects of extensive research because of the scientific importance and technical applications [1–3]. On tuning the photon energy in the soft x-ray region, one can excite selectively a specific atom or a specific site in a molecule. Inner-shell electrons of a particular element in a molecule can be excited selectively to a specific valence state or a Rydberg orbital below the core ionization threshold, or ejected into a shape resonance or a continuum above the ionization threshold. De-excitation of these core-excited or core-ionized molecules typically involves resonant Auger decay or normal Auger processes, producing multiply charged molecular ions that are unstable and that subsequently undergo dissociation. The intricate fragmentation dynamics of core-excited states of gaseous molecules and solid-state analogs attract broad interest [4–7].

Most experiments have involved measuring positive ions, whereas other fragmentation products, such as neutral fragments or negative ions [4–11], are less investigated. Neutral fragments might be detected for gaseous molecules and adsorbates on surfaces via core-level excitations [12–15]. Neutral photodissociation is difficult to investigate particularly for gaseous molecules; but, if the neutral fragments are in an excited state, dispersed fluorescence spectra prove to be a powerful tool for the investigation of neutral photodissociation of molecules with excitation. Ultraviolet-visible fluorescence can provide valuable information regarding the de-excitation and fragmentation of core-excited molecules through its capability to probe both neutral and ionic fragments [12,14,16].

Anion formation of molecules following valence-shell excitation is well studied. Under valence-shell excitation, one decay path of a molecular superexcited state is polar photodissociation to form an anion-cation pair that might then dissociate into a positive ion and a negative ion. For core-level excitation, the probability to produce ion-pair states of molecules that might yield an anion is diminished remarkably relative to valence-shell excitation. Dujardin *et al.* [17] first reported the observation of anion formation in the S 2*p* region of SO₂. The negative ion was presumed to be emitted from singly charged molecular-ion states produced by resonant Auger decay of core-excited states.

The detection of negative fragment ions is a powerful method of exposing high-lying molecular ion states from the relaxed core-excited states. Such high-lying molecular ion states might be weak in x-ray absorption spectra and positive-ion yield spectra but might appear as strong resonances in negative-ion yield spectra following core-level excitation [17,18]. Little research has been devoted to these high-lying molecular ion states and their role in ion desorption for molecular adsorbates on surfaces. Besides, the dissociation channels of core-excited molecules in the solid phase are strongly modified relative to the gaseous phase because of electronic interaction with a substrate or neighboring molecules in the solid phase [11,12]. To elucidate the dissociation dynamics of core-excited molecules, coordinated studies of gaseous-phase molecules and solid-state analogs are accordingly indispensable. There exist few reports of coordinated studies of anionic fragments and neutral fragments produced by inner-shell excitation of gaseous and condensed molecules.

The spectral properties of CCl₄ are imperative for its technical importance in the reactive ion etching of microelectronics. CCl₄ and halomethanes adsorbed on single-crystalline surfaces are model systems for studies of surface photochemistry. In this work, we investigated the dissociation dynamics of anionic and excited neutral fragments of gaseous CCl₄ and CCl₄ adsorbed on Si(100) ~90 K with variable coverage following excitation of Cl 2*p* electrons to various resonances

*Corresponding author: ktlu@nsrc.org.tw†Corresponding author: jmchen@nsrc.org.tw

on combining measurements of anionic photodissociation, x-ray absorption, and uv-visible dispersed fluorescence.

II. EXPERIMENTS

The experimental measurements were performed at the high-energy spherical grating monochromator (HSGM) beamline and the U5 undulator beamline coupled with a spherical grating monochromator of National Synchrotron Radiation Research Center (NSRRC) in Taiwan. For anionic dissociation measurements in a condensed phase, an ultrahigh-vacuum (UHV) chamber with a base pressure of $\sim 1 \times 10^{-10}$ Torr was used. Before installation in the UHV chamber, the substrate Si(100) crystal was treated with a hydrogen-peroxide-based immersion cleaning procedure to remove residual organic molecules and transition metals from cutting. The crystal was then mounted on a liquid nitrogen-cooled sample holder. The Si(100) surface was cleaned by repeated resistive heating to ~ 1100 °C under vacuum before the measurements. The highly pure CCl_4 (Merck, 99.9%) was degassed with several freeze-pump-thaw cycles before use. The vapor of CCl_4 was then condensed through a leak valve onto a Si(100) surface at ~ 90 K. Solid-phase x-ray absorption spectra were recorded in a total-electron yield (TEY) mode using a microchannel-plate detector. Negative ions were mass selected with a quadrupole mass spectrometer with an off-axis secondary electron multiplier (Balzers, QMA 410). The quadrupole detector was oriented perpendicular to the substrate surface, and photons were incident at an angle of 45° with respect to the substrate normal. The surface coverage was determined with thermal desorption spectra (TDS). The TDS spectra from $\text{CCl}_4/\text{Si}(100)$ show a single molecular desorption at ~ 139 K with an exposure 4 L or less. For an exposure above 4 L, an additional signal begins to appear at temperature ~ 132 K and its intensity increases with exposures. 4 L exposure of CCl_4 on Si(100) thus corresponds to one monolayer (ML).

To measure anionic photofragments in the gaseous phase, we formed an effusive molecular beam on expanding the gas through an orifice (diameter $50 \mu\text{m}$) into the experimental chamber. The pressure in this chamber was maintained at $\sim 2 \times 10^{-5}$ Torr. Negative fragment ions were selected by mass with a quadrupole mass filter and detected with an off-axis channel-electron multiplier (Hiden, EQS). To ensure that detected negative ions were produced in unimolecular processes, we measured anion-yield spectra at varied pressures of gas. To obtain satisfactory statistics, anion yield spectra were the sum of five recordings, each of which was separately normalized. Ultraviolet or visible fluorescence was dispersed with a 0.39 m spectrometer using a $f/1.5$ fused-silica extraction lens located normal to and in the plane of polarization of the synchrotron radiation. The fluorescence was detected with a photomultiplier tube (PMT) (Hamamatsu R928). During the measurement of dispersed fluorescence, the pressure in the effusive-beam chamber was kept at $\sim 9 \times 10^{-5}$ Torr. Gas-phase absorption spectra were measured with an ion chamber at pressure $\sim 1 \times 10^{-4}$ Torr.

To obtain the x-ray absorption spectrum at high resolution, the HSGM beamline was set to a photon resolution

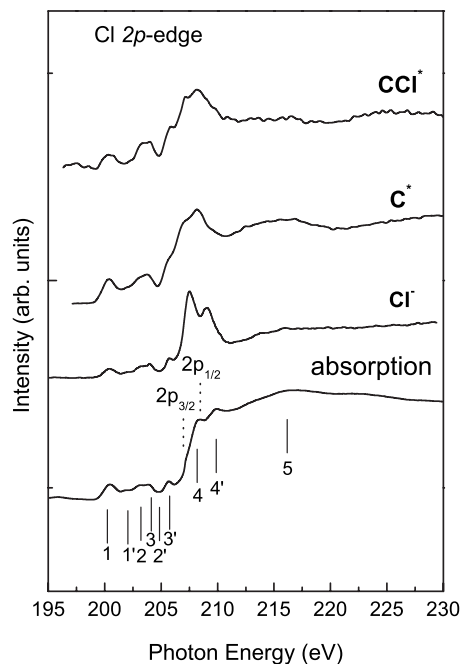


FIG. 1. Yields of Cl^- anion fragment and excited neutral fragments (C^* and CCl^*) from gaseous CCl_4 following Cl $2p$ core-level excitation, with the Cl L -edge x-ray absorption spectrum. The Cl ($2p_{3/2}$) and Cl ($2p_{1/2}$) ionization thresholds of gaseous CCl_4 (206.9 and 208.5 eV, respectively [20]) are marked with vertical dashed lines.

~ 0.1 eV at the Cl $2p$ edge. Because of small signal levels in measurements of dispersed fluorescence, the U5 undulator beamline was operated with a $100 \mu\text{m}$ entrance slit and a $300 \mu\text{m}$ exit slit (resolution ~ 0.3 eV at 200 eV), whereas the spectral resolution of the spectrometer was set to ~ 10 nm. The incident photon intensity (I_0) was monitored simultaneously with a Ni mesh located after the exit slit of the monochromator. All anion-yield spectra, x-ray absorption spectra, and fluorescence excitation spectra were normalized to the incident photon flux at the Cl $2p$ edge. The photon energies were calibrated within an accuracy of 0.1 eV using the Cl $2p$ absorption peak at 201.7 eV in gaseous SiCl_4 [19].

III. RESULTS AND DISCUSSION

The major product of anion fragments for gaseous CCl_4 via Cl $2p$ core-level excitation is Cl^- . We monitored also the uv-visible dispersed fluorescence of gaseous CCl_4 via Cl $2p$ core-level excitation. The main features in the dispersed fluorescence spectrum for photoionization of a Cl $2p$ electron of gaseous CCl_4 were identified as emission from excited CCl^{+*} ions ($A^1\Pi-X^1\Sigma^+$ at 240 nm), excited C^* atoms (at 240 and 254.9 nm), excited CCl^* fragments ($A^2\Delta-X^2\Pi$ at 278.2 nm), and excited Cl^{+*} ions (at 384.5, 480, and 521 nm) [15]. In Fig. 1, the Cl^- fragment yield for gaseous CCl_4 following Cl $2p$ core-level excitation is reproduced with the Cl L -edge x-ray absorption spectrum. The yields of excited neutral atomic C^* fragment (emission recorded at 254.9 nm) and excited neutral diatomic CCl^* fragment (emission recorded at 278.2 nm) as a function of photon energy in the

TABLE I. Energy positions and the assignments of absorption peaks in the Cl L -edge absorption spectra of gaseous CCl_4 [15,20]. The energies are expressed in eV.

Peak	Peak position	Assignment
1	200.3	$7a_1^*$
1	201.9	$7a_1^*$
2	202.9	$8t_2^*$
3	203.9	Rydberg state
2'	204.6	$8t_2^*$
3'	205.5	Rydberg state
4	208.3	Delay onset and shake-up
4'	209.9	Delay onset and shake-up
5	216	Shape resonance

Cl $2p$ edge of gaseous CCl_4 are depicted in Fig. 1 for comparison. The absorption features labeled 1 and 1' are assigned to the transition Cl $2p \rightarrow 7a_1^*$. The features labeled 2 and 2' correspond to the Cl $2p \rightarrow 8t_2^*$ excitations. Excitations of Cl $2p$ electrons to the Rydberg states are responsible for the absorptions labeled 3 and 3'. The absorptions labeled 4 and 4' are ascribed to a delayed onset of a Rydberg transition or a shake-up transition involving simultaneous excitation of a Cl $2p$ electron and a valence electron to unoccupied orbitals [15,20]. The broad peak at ~ 216 eV labeled 5 is attributed to a shape resonance. In Table I we list the energy positions and the assignments of absorption peaks in the Cl L -edge absorption spectra of gaseous CCl_4 .

Discernible in Fig. 1, the relative intensities of Cl^- yield spectrum and fluorescence excitation spectra of excited neutral fragments (C^* and CCl^*) differ notably from those of Cl L_{23} -edge absorption spectrum of gaseous CCl_4 . Excitations of the Cl $2p$ electrons to Rydberg orbitals and doubly excited states (absorptions labeled 3' and 4) near the Cl $2p$ ionization threshold of gaseous CCl_4 enhance both the excited neutral atomic fragments C^* and excited neutral diatomic fragments CCl^* , relative to the ratio of intensity of the corresponding transition to the core-to-valence excitation (absorption labeled 1) in the Cl L_{23} -edge X-ray absorption spectrum. In particular, excitations of Cl $2p$ electrons to higher Rydberg orbitals near the Cl $2p_{3/2}$ threshold (at ~ 207 eV) or doubly excited states (at ~ 208.2 eV) of gaseous CCl_4 remarkably enhance the production of excited neutral fragments. The Cl^- anion is significantly reinforced in the vicinity of the Cl $2p_{1/2,3/2}$ ionization threshold of gaseous CCl_4 . The maximum anion enhancement about 207.5 eV is just above the threshold, 206.9 eV, for Cl $2p_{3/2}$ ionization of gaseous CCl_4 . The Cl^- anion might thus be enhanced by the same dissociation channels that produced the excited neutral fragments.

The photoionization dynamics of an atom or a molecule near an inner-shell threshold and the subsequent relaxation are known to involve many-electron correlations. When the inner-shell electron of an atom or a molecule is ionized near the ionization threshold, a slowly moving photoelectron is ejected into the continuum. For atoms in a molecule of small or medium mass, the resulting core-ionized state relaxes pre-

dominantly via an Auger decay and a rapid Auger electron is emitted. The Coulomb interaction between a slowly moving photoelectron and a more energetic Auger electron, a so-called postcollision interaction (PCI), causes an energy loss of the slow photoelectron and a corresponding gain of energy of the Auger electron. The postcollision interaction manifests itself through changes in ion-yield spectra. The PCI effect is well studied for free atoms and molecules [21–28].

The resonant core-excited states of an atom or a molecule with an excited electron in unoccupied states decay predominantly by a spectator or participant Auger transition [29]. The spectator Auger decay yields a two-hole one-electron ($2h1e$) final state in which two holes are formed in valence orbitals and one electron is excited into an antibonding valence orbital or a Rydberg orbital. For excitation of a specific core electron of an atom or a molecule into the lowest unoccupied Rydberg states, the resonant Auger processes are dominated by the spectator Auger decay; i.e., the excited electron remains in the same Rydberg orbital during the decay. For excitations to higher Rydberg states, the shake-modified resonant Auger transition with an excitation of the outer electron to a valence shell or a Rydberg orbital, so-called shake up, plays a crucial role in resonant Auger processes [30–35]. The shake-modified resonant Auger decay yields multiple-hole multiple-electron (mhme) final states. According to resonant photoemission studies of gaseous CCl_4 , the width of spectator Auger peaks via higher Rydberg excitations at the peak labeled 3' (FWHM ~ 10 eV) near the Cl $2p$ ionization threshold is much broader than that via valence-band excitation (FWHM ~ 5 eV) and the width of a normal Auger peak (FWHM ~ 7 eV), likely due to contributions of shake-up or shake-down of spectator Auger electrons at higher Rydberg states [15].

In contrast, when the molecule is photoionized just above the specific core-shell ionization threshold, the slowly moving photoelectron is still near the molecular ion when Auger decay occurs. Through the postcollision interaction, the slow photoelectron is retarded and can become recaptured by the molecular ion into a Rydberg orbital, so-called shake down. The photoelectron recapture results in singly charged ions in high- n Rydberg states. The gradual evolution of a transition from the regime of shake-up modified resonant Auger decay induced by core-level excitation below the threshold to the regime of PCI-mediated shake-down just above the threshold has been studied both theoretically and experimentally for several systems [36–41].

Shake-up modified resonant Auger decay and PCI-mediated shake down near the ionization threshold accordingly produce highly excited ionic Rydberg states, efficiently producing excited neutral fragments, because the wave function of a diffuse Rydberg electron has less overlap with the molecular-ion core; consequently the $2h1e$ or mhme states dissociate to produce the excited-state fragments before the excited Rydberg electron can relax. Recapture of a PCI-mediated photoelectron increases the probability of capture by the departing Cl atom during dissociation and then enhances the Cl^- yield near the Cl $2p$ ionization threshold of gaseous CCl_4 . Similar observations are reported for several small molecules following core-level excitation [14,42–47]. The detection of excited neutral particles and anion frag-

TABLE II. Proposed mechanisms for the enhanced production of anionic and excited neutral fragments of gaseous CCl_4 following Cl $2p$ excitation.

Enhanced fragment yields	Excitation	Proposed mechanisms
Excited neutral fragments (C^* and CCl^*)	High Rydberg states	Shake-up modified resonant Auger decay and/or PCI-mediated shake-down
Anionic fragments (Cl^-)	In the vicinity of the ionization threshold	PCI-mediated photoelectron recapture

ments is demonstrated to be a sensitive probe for investigating shake-modified resonant Auger decay, doubly excited states embedded in core-shell ionization continua, and PCI dynamics [42–49]. In Table II, we summarized the proposed mechanisms for the enhanced production of anionic and excited neutral fragments of gaseous CCl_4 following Cl $2p$ excitation.

As noted from Fig. 1, a prominent production of anion yield in the shape resonance region of Cl $2p$ edge of gaseous CCl_4 is observed, similar to other large molecules (SF_6 , SiF_4 , and SiCl_4), and at variance with many smaller molecules (CO , CO_2 , NO , and N_2O) for which the shape resonance is almost completely suppressed [49–54]. Many authors showed that multiple scattering of photoelectrons by neighboring atoms is crucial in interpreting the shape resonance features in the x-ray absorption spectrum, particularly for large molecules and the solid phase [55–57]. Accordingly, the shape resonance of the Cl $2p$ edge of gaseous CCl_4 shows a more delocalized character, and the resonant intensity of anions is greater in the shape resonance regime.

Cl^- was the only anion observed in the negative-ion desorption of $\text{CCl}_4/\text{Si}(100)$ following Cl $2p$ core-level excitation. To elucidate the mechanism of negative-ion desorption, we measured the Cl^- yield as a function of CCl_4 exposure on Si(100) at ~ 90 K, as shown in Fig. 2. Especially noteworthy there is that the Cl $2p \rightarrow 7a_1^*$ excitation notably enhances the Cl^- desorption yield at submonolayer (1 L), as shown in the insert of Fig. 2. We found also that the Cl^- yield at a shape resonance (~ 216 eV) shows a monotonic increase with CCl_4 exposure and is closely correlated with electron yield. The possible desorption mechanism of Cl^- from $\text{CCl}_4/\text{Si}(100)$ at shape resonance was hence likely due to dissociative attachment to molecules of secondary electrons produced by photoabsorption of molecular adsorbates. This desorption mechanism was called dissociative electron attachment (DEA) [58].

If the enhanced Cl^- yield at the $7a_1^*$ resonances is due to a DEA process, the Cl^- yield at the $7a_1^*$ resonance would be expected to show a trend like that at the shape resonance because the energy distribution of the secondary electrons becomes indistinguishable for photoexcitation at a shape resonance and at other photon energies. The Cl^- yield at the $7a_1^*$ resonance is hence expected to increase monotonically with CCl_4 exposure. In contrast, the Cl^- yield at the $7a_1^*$ resonance shows a notable enhancement at submonolayer and exhibits a nonlinear change with CCl_4 exposure, as shown in Fig. 2. Moreover, the observed $7a_1^*$ resonances have the same energies and widths between Cl^- yield and TEY spectra. We therefore propose that the enhanced Cl^-

yield from $\text{CCl}_4/\text{Si}(100)$ at the $7a_1^*$ resonance is due not to DEA but to a unimolecular process.

Based on resonant photoemission of CCl_4 , the spectator Auger transitions prevail predominantly following the Cl $2p$ core-to-valence and Cl $2p$ core-to-Rydberg excitations, producing an excited ionized state of the parent molecule with the originally excited electron acting as a spectator. Some highly excited molecular-ion states might decompose into an ion-pair channel producing a negative ion and an associated doubly charged fragment. Negative-ion formation might presumably originate from some high-lying molecular-ion states that are predissociated by an ion-pair or that directly dissociate [17]. Based on a model proposed by Dujardin *et al.*, the intensities of resonances in the negative-ion yield spectrum are closely correlated with the probability of spectator electrons becoming attached to the electronegative atom during fragmentation of the molecules [17]. From multiple-scattering $X\alpha$ calculations on CCl_4 , the spectator electron in the $7a_1^*$ orbital is localized slightly more at the Cl side, whereas the $8t_2^*$ orbital is delocalized between Cl and C atoms [59]. The Cl $2p \rightarrow 7a_1^*$ excitation is thus expected to enhance the Cl^- yield at a small coverage, relative to transi-

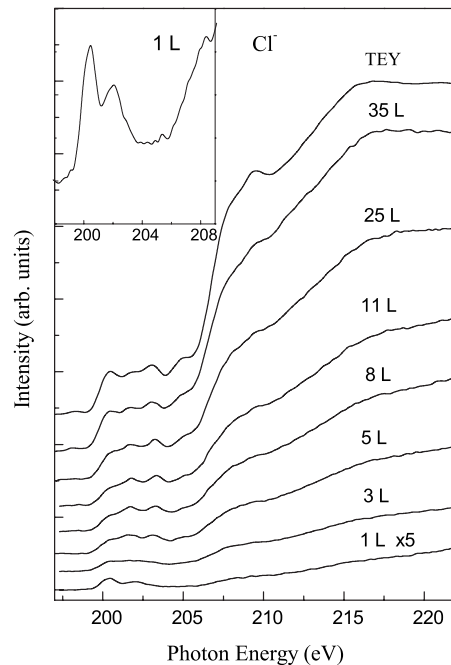


FIG. 2. Cl^- yield spectra of $\text{CCl}_4/\text{Si}(100)$ at ~ 90 K with variable coverage following Cl $2p$ core-level excitation, with the Cl L -edge TEY spectrum of solid CCl_4 . The inset shows an enlarged pre-edge regime of the Cl^- yield spectrum at 1 L.

tions, $\text{Cl } 2p \rightarrow 8t_2^*$ and $\text{Cl } 2p \rightarrow \text{Rydberg}$ states, as observed in Fig. 2.

We compare anion formation between condensed CCl_4 and gaseous CCl_4 following $\text{Cl } 2p$ core-level excitation. The $\text{Cl } 2p \rightarrow 7a_1^*$ excitation for $\text{CCl}_4/\text{Si}(100)$ at ~ 90 K enhanced the Cl^- desorption yield at a submonolayer level, whereas the Cl^- anion was significantly reinforced near the $\text{Cl } 2p_{1/2,3/2}$ ionization threshold of gaseous CCl_4 . At a small coverage of $\text{CCl}_4/\text{Si}(100)$, polarization induced by the substrate lowers the potential-energy surface of the high-lying singly charged molecular-ion state and imparts translational energy to Cl^- , accordingly permitting it to escape from its image potential [60]. At a large coverage, the Cl^- yield spectrum for $\text{CCl}_4/\text{Si}(100)$ is dominated by dissociative electron attachment and thus strongly resembles the $\text{Cl } L_{2,3}$ -edge x-ray absorption spectrum. For the gaseous phase, the notably enhanced Cl^- anion in the vicinity of the $\text{Cl } 2p_{1/2,3/2}$ ionization threshold of CCl_4 is mediated by the PCI-mediated photoelectron recapture.

The detailed dissociation dynamics for the formation of anionic and excited neutral fragments require sophisticated calculations of potential-energy curves for high-lying molecular CCl_4^+ states and a comprehensive analysis of the resonant Auger spectra of CCl_4 at high resolution for high Rydberg resonances near the $\text{Cl } 2p$ ionization threshold [61]. An intricate measurement such as threshold electron-fluorescence coincidence spectra is crucial to elucidate these detailed dissociation mechanisms [62]. However, the potential energy surfaces of a large molecule such as CCl_4 , particularly for high-lying molecular CCl_4^+ states, are quite complex to present-day theoretical calculation. Hopefully, our results will stimulate further theoretical development in the dissociation dynamics for excited neutral and anionic fragments of gaseous molecules near the ionization threshold.

IV. CONCLUSION

We investigated the dissociation dynamics of anionic and excited neutral fragments of gaseous CCl_4 and CCl_4 adsorbed on $\text{Si}(100)$ ~ 90 K with variable coverage following $\text{Cl } 2p$ core-level excitations on combining measurements of photon-induced anionic dissociation, x-ray absorption, and uv-visible dispersed fluorescence. The $\text{Cl } 2p \rightarrow 7a_1^*$ excitation for $\text{CCl}_4/\text{Si}(100)$ enhances the Cl^- desorption yield at a submonolayer level, whereas the Cl^- anion is significantly enhanced near the $\text{Cl } 2p_{1/2,3/2}$ ionization threshold of gaseous CCl_4 . The transitions of core electrons to high Rydberg states near $\text{Cl } 2p$ ionization thresholds and doubly excited states of gaseous CCl_4 greatly enhance excited neutral fragments (C^* and CCl^*), originating from shake-modified resonant Auger decay or/and postcollision interaction. The notably enhanced Cl^- anion near the $\text{Cl } 2p_{1/2,3/2}$ ionization threshold of gaseous CCl_4 is affected by PCI-mediated photoelectron recapture. The resonant enhancement of the Cl^- yield at the $7a_1^*$ resonance in the $\text{Cl } 2p$ edge at a submonolayer level occurs through a formation of high-lying molecular-ion states for CCl_4 adsorbed on a Si surface, mediated by polarization induced by the substrate. Our experimental results provide important insight concerning the roles and relative importance of dissociative electron attachment and high-lying molecular-ion states on dissociation dynamics of negative ion for adsorbates on surfaces. These complementary results provide insight into the anionic and excited neutral fragmentations of gaseous molecules and solid-state analogs via core-level excitation.

ACKNOWLEDGMENTS

We thank the NSRRC staff for their technical support. NSRRC and National Science Council of the Republic of China (under Grants No. NSC 96-2113-M-213-009 and No. 96-2113-M-213-007) supported this research.

-
- [1] T. Urisu and H. Kyuragi, *J. Vac. Sci. Technol. B* **5**, 1436 (1987).
 [2] R. A. Rosenberg, S. P. Frigo, and J. K. Simons, *Appl. Surf. Sci.* **79-80**, 47 (1994).
 [3] K. Ueda, S. Tanaka, Y. Shimizu, Y. Muramatsu, H. Chiba, T. Hayaishi, M. Kitajima, and H. Tanaka, *Phys. Rev. Lett.* **85**, 3129 (2000).
 [4] Y. Baba, *Low Temp. Phys.* **29**, 228 (2003) and references therein.
 [5] S. Svensson, *J. Phys. B* **38**, S821 (2005) and references therein.
 [6] K. Ueda, *J. Phys. B* **36**, R1 (2003) and references therein.
 [7] K. Ueda and J. H. D. Eland, *J. Phys. B* **38**, S839 (2005).
 [8] S. Nagaoka, K. Mase, M. Nagasono, S. Tanaka, T. Urisu, and J. Ohshita, *J. Chem. Phys.* **107**, 10751 (1997).
 [9] M. C. K. Tinone, K. Tanaka, J. Maruyama, N. Ueno, M. Imamura, and N. Matsubayashi, *J. Chem. Phys.* **100**, 5988 (1994).
 [10] X. J. Liu, G. Prümper, E. Kukk, R. Sankari, M. Hoshino, C. Makochekanwa, M. Kitajima, H. Tanaka, H. Yoshida, Y. Tamenori, and K. Ueda, *Phys. Rev. A* **72**, 042704 (2005).
 [11] S. Nagaoka, K. Mase, and I. Kayano, *Trends Chem. Phys.* **6**, 1 (1997).
 [12] J. M. Chen, K. T. Lu, J. M. Lee, C. I. Ma, and Y. Y. Lee, *Phys. Rev. Lett.* **92**, 243002 (2004).
 [13] M. Meyer, S. Aloise, and A. N. Grum-Grzhimailo, *Phys. Rev. Lett.* **88**, 223001 (2002).
 [14] R. Romberg, N. Heckmair, S. P. Frigo, A. Ogurtsov, D. Menzel, and P. Feulner, *Phys. Rev. Lett.* **84**, 374 (2000).
 [15] K. T. Lu, J. M. Chen, J. M. Lee, C. K. Chen, T. L. Chou, and H. C. Chen, *New J. Phys.* **10**, 053009 (2008).
 [16] J. M. Chen, K. T. Lu, J. M. Lee, S. C. Ho, and H. W. Chang, *Phys. Rev. A* **72**, 032706 (2005).
 [17] G. Dujardin, L. Hellner, B. J. Olsson, M. J. Besnard-Ramage, and A. Dadouch, *Phys. Rev. Lett.* **62**, 745 (1989).
 [18] J. M. Chen and K. T. Lu, *Phys. Rev. Lett.* **86**, 3176 (2001).
 [19] J. M. Chen, R. Klauser, S. C. Yang, and C. R. Wen, *Chem.*

- Phys. Lett. **246**, 285 (1995).
- [20] A. P. Hitchcock and C. E. Brion, *J. Electron Spectrosc. Relat. Phenom.* **14**, 417 (1978).
- [21] A. De Fanis, G. Prümper, U. Hergenhahn, M. Oura, M. Kitajima, T. Tanaka, H. Tanaka, S. Fritzsche, N. M. Kabachnik, and K. Ueda, *Phys. Rev. A* **70**, 040702(R) (2004).
- [22] R. Hentges, N. Müller, J. Viefhaus, U. Heinzmann, and U. Becker, *J. Phys. B* **37**, L267 (2004).
- [23] J. Tulkki, T. Åberg, S. B. Whitfield, and B. Crasemann, *Phys. Rev. A* **41**, 181 (1990).
- [24] J. A. R. Samson, W. C. Stolte, Z. X. He, J. N. Cutler, and D. L. Hansen, *Phys. Rev. A* **54**, 2099 (1996).
- [25] W. C. Stolte, Y. Lu, J. A. R. Samson, O. Hemmers, D. L. Hansen, S. B. Whitfield, H. Wang, P. Glans, and D. W. Lindle, *J. Phys. B* **30**, 4489 (1997).
- [26] J. A. R. Samson, Y. Lu, and W. C. Stolte, *Phys. Rev. A* **56**, R2530 (1997).
- [27] V. Schmidt, N. Sandner, W. Mehlhorn, M. Y. Adam, and F. Wuilleumier, *Phys. Rev. Lett.* **38**, 63 (1977).
- [28] G. B. Armen and J. C. Levin, *Phys. Rev. A* **56**, 3734 (1997).
- [29] S. Aksela, K. H. Tan, H. Aksela, and G. M. Bancroft, *Phys. Rev. A* **33**, 258 (1986).
- [30] O. P. Sairanen, H. Aksela, S. Aksela, J. Mursu, A. Kivimäki, A. Naves de Brito, E. Nömmiste, S. J. Osborne, A. Ausmees, and S. Svensson, *J. Phys. B* **28**, 4509 (1995).
- [31] J. Jauhiainen, H. Aksela, O. P. Sairanen, E. Nömmiste, and S. Aksela, *J. Phys. B* **29**, 3385 (1996).
- [32] H. Aksela, S. Aksela, H. Pulkkinen, G. M. Bancroft, and K. H. Tan, *Phys. Rev. A* **37**, 1798 (1988).
- [33] R. Püttner, Y. F. Hu, G. M. Bancroft, A. Kivimäki, M. Jurvan-suu, H. Aksela, and S. Aksela, *Phys. Rev. A* **77**, 032705 (2008).
- [34] D. Čubrić, A. A. Wills, E. Sokell, J. Comer, and M. A. Mac-donald, *J. Phys. B* **26**, 4425 (1993).
- [35] S. B. Whitfield, J. Tulkki, and T. Åberg, *Phys. Rev. A* **44**, R6983 (1991).
- [36] G. B. Avaldi, R. I. Hall, G. Dawber, P. M. Rutter, and G. C. King, *J. Phys. B* **24**, 427 (1991).
- [37] G. B. Armen, T. Åberg, J. C. Levin, B. Crasemann, M. H. Chen, G. E. Ice, and G. S. Brown, *Phys. Rev. Lett.* **54**, 1142 (1985).
- [38] J. A. de Gouw, J. van Eck, J. van der Weg, and H. G. M. Heideman, *J. Phys. B* **28**, 1761 (1995).
- [39] T. Åberg, *Phys. Scr.* **T41**, 71 (1992).
- [40] H. R. Sadeghpour, J. L. Bohn, M. J. Cavagnero, B. D. Esryk, I. I. Fabrikant, J. H. Macek, and A. R. P. Rau, *J. Phys. B* **33**, R93 (2000).
- [41] H. Aksela, M. Kivilompolo, E. Nömmiste, and S. Aksela, *Phys. Rev. Lett.* **79**, 4970 (1997).
- [42] D. L. Hansen, G. B. Armen, M. E. Arrasate, J. Cotter, G. R. Fisher, K. T. Leung, J. C. Levin, R. Martin, P. Neill, R. C. C. Perera, I. A. Sellin, M. Simon, Y. Uehara, B. Vanderford, S. B. Whitfield, and D. W. Lindle, *Phys. Rev. A* **57**, R4090 (1998).
- [43] D. L. Hansen, M. E. Arrasate, J. Cotter, G. R. Fisher, O. Hemmers, K. T. Leung, J. C. Levin, R. Martin, P. Neill, R. C. C. Perera, I. A. Sellin, M. Simon, Y. Uehara, B. Vanderford, S. B. Whitfield, and D. W. Lindle, *Phys. Rev. A* **58**, 3757 (1998).
- [44] J. M. Chen, K. T. Lu, J. M. Lee, T. L. Chou, H. C. Chen, S. A. Chen, S. C. Haw, and T. H. Chen, *New J. Phys.* **10**, 103010 (2008).
- [45] M. Meyer, P. O’Keeffe, J. Plenge, R. Flesch, and E. Rühla, *J. Chem. Phys.* **125**, 214306 (2006).
- [46] G. Vall-Ilosera, E. Melero García, A. Kivimäki, E. Rachlew, M. Coreno, M. de Simone, R. Richter, and K. C. Prince, *Phys. Chem. Chem. Phys.* **9**, 389 (2007).
- [47] Y. Hikosaka, P. Lablanquie, and E. Shigemasa, *J. Phys. B* **38**, 3597 (2005).
- [48] A. Kivimäki, M. de Simone, M. Coreno, V. Feyer, E. M. García, J. Á. Ruiz, R. Richter, and K. C. Prince, *Phys. Rev. A* **75**, 014503 (2007).
- [49] W. C. Stolte, D. L. Hansen, M. N. Piancastelli, I. Dominguez Lopez, A. Rizvi, O. Hemmers, H. Wang, A. S. Schlachter, M. S. Lubell, and D. W. Lindle, *Phys. Rev. Lett.* **86**, 4504 (2001).
- [50] S. W. J. Scully, R. A. Mackie, R. Browning, K. F. Dunn, and C. J. Latimer, *J. Phys. B* **35**, 2703 (2002).
- [51] M. N. Piancastelli, W. C. Stolte, R. Guillemin, A. Wolska, and D. W. Lindle, *J. Chem. Phys.* **128**, 134309 (2008).
- [52] S.-W. Yu, W. C. Stolte, G. Öhrwall, R. Guillemin, M. N. Piancastelli, and D. W. Lindle, *J. Phys. B* **36**, 1255 (2003).
- [53] L. T. N. Dang, W. C. Stolte, G. Öhrwall, M. M. Sant’Anna, I. Dominguez Lopez, A. S. Schlachter, and D. W. Lindle, *Chem. Phys.* **289**, 45 (2003).
- [54] S.-W. Yu, W. C. Stolte, R. Guillemin, G. Öhrwall, I. C. Tran, M. N. Piancastelli, R. Feng, and D. W. Lindle, *J. Phys. B* **37**, 3583 (2004).
- [55] A. Bianconi, A. Di Cicco, N. V. Pavel, M. Benfatto, A. Marcelli, C. R. Natoli, P. Pianetta, and J. Woicik, *Phys. Rev. B* **36**, 6426 (1987).
- [56] J. M. Chen, J. K. Simons, K. H. Tan, and R. A. Rosenberg, *Phys. Rev. B* **48**, 10047 (1993).
- [57] S. Bodeur, P. Millie, and I. Nenner, *Phys. Rev. A* **41**, 252 (1990).
- [58] L. G. Christophorou, D. L. McCorkle, and A. A. Christodoulides, in *Electron-molecule Interactions and their Applications*, edited by L. G. Christophorou (Academic, Orlando, 1984), Vol. 1.
- [59] J. A. Tossell and J. W. Davenport, *J. Chem. Phys.* **80**, 813 (1984).
- [60] P. Ayotte, J. Gamache, A. D. Bass, I. I. Fabrikant, and L. Sanche, *J. Phys. Chem.* **106**, 749 (1997).
- [61] M. Kitajima, R. Püttner, S. L. Sorensen, T. Tanaka, M. Hoshino, H. Fukuzawa, A. De Fanis, Y. Tamenori, R. Sankari, M. N. Piancastelli, H. Tanaka, and K. Ueda, *Phys. Rev. A* **78**, 033422 (2008).
- [62] E. Rühl and R. Flesch, *J. Chem. Phys.* **121**, 5322 (2004).